A New Combined Computational and NMR-Spectroscopical Strategy for the Identification of Additional Conformational Constraints of the Bound Ligand in an Aprotic Solvent

Hans-Christian Siebert,[a] Sabine André,[a] Juan Luis Asensio,[b]
Francisco Javier Cañada,[b] Xin Dong,[a] Juan Felix Espinosa,[b] Martin Frank,[c]
Martine Gilleron,[d] Herbert Kaltner,[a] Tibor Kozár,[e] Nicolai V. Bovin,[f]
Claus-Wilhelm von der Lieth,[c] Johannes F. G. Vliegenthart,[g]
Jesús Jiménez-Barbero,[b] and Hans-Joachim Gabius*[a]

This study documents the feasibility of switching to an aprotic medium in sugar receptor research. The solvent change offers additional insights into mechanistic details of receptor–carbohydrate ligand interactions. If a receptor retained binding capacity in an aprotic medium, solvent-exchangeable protons of the ligand would not undergo transfer and could act as additional sensors, thus improving the level of reliability in conformational analysis. To probe this possibility, we first focused on hevein, the smallest lectin found in nature. The NMR-spectroscopic measurements verified complexation, albeit with progressively reduced affinity by more than 1.5 orders of magnitude, in mixtures of up to 50% dimethyl sulfoxide (DMSO). Since hevein lacks the compact β-strand arrangement of other sugar receptors, such a structural motif may confer enhanced resistance to solvent exchange. Two settings of solid-phase activity assays proved this assumption for three types of α- and/or β-galactoside-binding proteins, that is, a human immunoglobulin G (IgG) subfraction, the mistletoe lectin, and a member of the galectin family of animal lectins. Computer-assisted calculations and NMR experiments also revealed no conspicuous impact of the solvent on the conformational properties of the tested ligands. To define all possible nuclear Overhauser effect (NOE) contacts in a certain conformation and to predict involvement of exchangeable protons, we established a new screening protocol applicable during a given molecular dynamics (MD) trajectory and calculated population densities of distinct contacts. Experimentally, transferred NOE (tr-NOE) experiments with IgG molecules and the disaccharide Gal′α1-3Galβ1-R in DMSO as solvent disclosed that such an additional crosspeak, that is, Gal′ OH2 – Gal OH4, was even detectable for the bound ligand under conditions in which spin diffusion effects are suppressed. Further measurements with the plant lectin and galectins confirmed line broadening of ligand signals and gave access to characteristic crosspeaks in the aprotic solvent and its mixtures with water. Our combined biochemical, computational, and NMR-spectroscopical strategy is expected to contribute notably to the precise elucidation of the geometry of ligands bound to compactly folded sugar receptors and of the role of water molecules in protein–ligand (carbohydrate) recognition, with relevance to areas beyond the glycosciences.

KEYWORDS:

carbohydrates · immunoglobulins · lectins · molecular dynamics · NMR spectroscopy

[a] Prof. Dr. H.-J. Gabius, Priv.-Doz. Dr. Dr. habil. H.-C. Siebert, Dr. S. André, Dr. X. Dong, Priv.-Doz. Dr. Dr. habil. H. Kaltner
Institut für Physiologische Chemie, Tierärztliche Fakultät
Ludwig-Maximilians-Universität
Veterinärstrasse 13, 80539 München (Germany)
Fax: (+49) 89-21802508
E-mail: gabius@tiph.vetmed.uni-muenchen.de

[b] Dr. J. L. Asensio, Dr. F. J. Cañada, Dr. J. F. Espinosa, Dr. J. Jiménez-Barbero
Consejo Superior de Investigaciones Cientificas
Instituto de Química Orgánica
Juan de la Cierva 3, 28006 Madrid (Spain)

[c] Dr. M. Frank, Dr. C.-W. von der Lieth
Deutsches Krebsforschungszentrum, Zentrale Spektroskopie
Im Neuenheimer Feld 280, 69120 Heidelberg (Germany)

[d] Dr. M. Gilleron
Institut de Pharmacologie et de Biologie Structurale du CNRS
205 route de Narbonne, 31077 Toulouse Cédex (France)

[e] Dr. T. Kozár
GlycoDesign Inc.
480 University Avenue, Toronto, ON M5G 1V2 (Canada)

[f] Dr. N. V. Bovin
Shemyakin Institute of Bioorganic Chemistry
Russian Academy of Sciences
ul. Miklukho-Maklaya 16/10, Moscow (Russia)

[g] Prof. Dr. J. F. G. Vliegenthart
Bijvoet Center for Biomolecular Research
Department of Bio-Organic Chemistry, Utrecht University
P.O. Box 80.075, 3508 TB Utrecht (The Netherlands)

Supporting information for this article is available on the WWW under http://www.wiley-vch.de/home/chembiochem/ or from the author.

Introduction

Based on theoretical considerations, oligosaccharides surpass by far any other class of biomolecules in their capacity to store biological information.[1] In the interplay with lectins, messages from distinct parts of glycan chains are decoded and transmitted into cellular responses such as cell adhesion or growth regulation.[2–6] This type of molecular recognition and insights into its intimate details are essential to pinpoint structural elements responsible for facilitating distinct processes at the cellular level. On this basis, it is possible to design drugs that rationally interfere, for example, with the unwanted lectin-mediated docking of infectious bacteria.[7–9] In addition to knowledge of the properties of the receptor and the ligand, an understanding of the thermodynamic parameters linked to the solvent during association will have a pronounced impact on attaining rational drug design.

To contribute notably to the ongoing discussion on the nature of the driving forces towards the rendezvous between a lectin and its cognate oligosaccharides,[10–13] exploitation of NMR spectroscopy, especially the monitoring of tr-NOE** effects in receptor–ligand mixtures, has proven to be valuable in combination with computer-assisted molecular mechanics and dynamics calculations.[14–21] However, the chemical nature of the ligand severely restricts the extent of readily accessible information on interresidual magnetization transfer in the physiological environment. Usually, protons of ring C—H bonds act as sensors in this technique, because the high rate of exchange of protons from hydroxy groups with solvent protons in water places a barrier to obtaining information about ligand topology from hydroxy groups.

To overcome this problem, the temperature dependence of the proton exchange affords an opportunity to suppress its troublesome consequences at least for the free ligand. Kinetic suppression of this process has been rendered feasible with a drastic temperature decrease substantially below 0 °C by either adding an appropriate, freezing-point-reducing solvent[22–25] or using supercooled aqueous solutions,[26] with the inherent limitations of this approach for monitoring of complexes being obvious. When physiological conditions are to be maintained, the geometry of water-exchangeable protons of a ^{13}C-labeled ligand associated to a lectin (i.e., the trimeric fragment of rat serum mannan-binding lectin as model) was inferred by cross-relaxation to nonexchangeable, ^{13}C-coupled ring protons under conditions of selective water inversion.[27] Herein, we explore the possibility to obtain structural information, at least in distinct cases, on these rapidly exchangeable protons by using an aprotic solvent.

Our investigation of sugar binding in an aprotic dipolar solvent was based on two independent lines of evidence, dealing separately with the carbohydrate and the protein parts of this recognition system. Since a protic solvent will immediately enable proton exchange to occur with loss of spectral resolution, it was straightforward to prevent this process by withdrawing solvent protons. The assumption to be able to

record sharp resonance lines from carbohydrates dissolved in aprotic media such as DMSO was initially ascertained by Casu et al.[28] This technique has also become instrumental for glycan analysis of glycolipids which will not form micelles in organic solvents.[29] Although the relative chemical shifts of carbohydrate proton signals in water and DMSO can be quite different, as for example determined for the histo-blood group A-tetra- and H-hexasaccharides, the conformations of these oligosaccharides were essentially insensitive to the solvent change.[30] A further indispensable prerequisite to proceed along this line, that is, solubility of proteins, is also met, because various proteins are indeed soluble in DMSO.[31, 32] Primarily, enzymes have so far been the target for such experiments owing to the promise of potential biotechnological applications.[33, 34] Despite the documentation of maintenance of at least a certain level of activity of several enzymes in aprotic solvents, the harmful effect of DMSO on tertiary and even secondary structures can severely impede the extension of NMR spectroscopic measurements from free carbohydrates to lectin–ligand complexes.[33, 35–39]

Supported by computational calculations and solid-phase activity assays to reveal whether the change of environment is compatible with retaining activity for a lectin or a carbohydrate-binding immunoglobulin, we demonstrate applicability and limits of this approach for various sugar receptors. Starting with hevein, whose small size has already enabled complete assignment of signals and detailed MD simulations,[40–43] corresponding NMR measurements are suitable to provide information on the sensitivity of its carbohydrate-binding activity to the presence of DMSO. Since the untypically small size of hevein will preclude generalizations for other sugar receptors with different folding patterns,[44] it was essential to examine the effect of the aprotic solvent on three classes of galactoside-binding proteins. Based on positive activity assays in two very sensitive biochemical test systems, our NMR measurements for two unrelated types of galactoside-binding plant and animal lectins (mistletoe lectin; mammalian and avian galectins) and a human immunoglobulin G subfraction are designed to answer the question whether this approach to monitor sugar binding in DMSO can lead to the acquisition of new information on ligand topology after association to the binding site. In addition, we present the application of a new screening protocol for profiling interproton distances of free ligands and detecting contacts involving water-exchangeable protons in MD simulations. These data are compared to the actual experimental results, thereby underscoring the predictive value of this new screening protocol.

Results and Discussion

NMR analysis of hevein and hevein–ligand complexes in pure DMSO and DMSO/water mixtures

NOESY-NMR data were acquired under different experimental conditions and in the course of titration NMR experiments. In detail, 1D and 2D spectra for hevein in [D$_6$]DMSO or [D$_6$]DMSO/H$_2$O mixtures were recorded and analyzed, as described for hevein dissolved in pure D$_2$O or H$_2$O. First, a freeze-dried sample containing a 1:4 (molar ratio) mixture of hevein and *N,N',N''*-triacetylchitotriose was dissolved in DMSO. The 1D proton

spectrum of hevein in pure [D$_6$]DMSO was well resolved with sharp resonance signals (see Supporting Information). 2D TOCSY and 2D NOESY NMR experiments provided information on structural aspects of the lectin in the aprotic solvent. The absence of characteristic signals in the fingerprint region[45] and the lack of dispersion indicated that well-defined secondary and tertiary structures are not present anymore when the protein is exposed to the aprotic solvent. For example, the aliphatic region of the TOCSY spectrum revealed no dispersion. The Cys 18 and Cys 24 α as well as the Gln 20 γ signals disappeared. These key proton signals are indicative of the integrity of hevein's native conformation in water.[40, 42] Similar results were obtained from scrutinizing the fingerprint region of the corresponding NOESY spectrum. Evidently, this lectin, which lacks a compact β-strand topology due to its small size, is subjected to a rather severe change of its structure that even affects elements of the secondary structure. Monitoring of 1D spectra of hevein in the presence of *N,N'*-diacetylchitobiose or *N,N',N''*-triacetylchito-triose in pure [D$_6$]DMSO solution addressed the issue whether this lectin retains binding activity in this solvent. An indication for line broadening of hevein or ligand signals from protons relevant for the binding process, a hint for association to the protein, was not detectable. This finding argues in favor of a complete loss of binding specificity by switching the solvent in the case of this small lectin. It is unknown to what extent the DMSO concentration in water can be increased before being detrimental to this lectin. To answer this question, the experimental assessment of signal characteristics in the presence of increasing concentrations of aprotic solvent and of the binding affinity in mixtures were required. Monitoring of formation of hevein – *N,N',N''*-triacetylchitotriose complexes was performed by NMR-controlled titration studies in mixtures of [D$_6$]DMSO and H$_2$O. The results of these measurements underscored that the presence of an aprotic solvent ([D$_6$]DMSO) in H$_2$O can well be tolerated by the lectin (Figure 1 a, b, c).

The alteration of signals from the aromatic part of the hevein spectrum in different mixtures of [D$_6$]DMSO and H$_2$O (5:95, 10:90, 15:85, and 20:80; v/v) is shown in Figure 1 a. Even at a ratio of [D$_6$]DMSO to H$_2$O of 20:80 the solution structure of hevein observed in pure water by NMR spectroscopy was still largely maintained. The presence of the organic solvent was yet inferable by certain alterations in the spectrum. The signals of the NH1 protons of Trp 21 and Trp 23 showed an approximately linear correlation between chemical shift and [D$_6$]DMSO concentration in the downfield direction (to higher ppm values). Other peaks (e.g., the NH and the γ proton signals of Gln 20) were also sensitive to the presence of [D$_6$]DMSO, broadening the experimental basis for the given conclusion. Since these measurements provided a rather qualitative insight into the changes of the receptor properties, a titration study with a fixed concentration of the protein and stepwise additions of *N,N',N''*-triacetylchitotriose was performed. This series of experiments is the logical extension of the previous study in water as solvent, which defined the K_b value of this protein – carbohydrate interaction to be 11 558 ± 2000 M^{-1} at $T = 298$ K.[40, 42]

Our NMR titration study with hevein and *N,N',N''*-triacetylchitotriose was carried out in mixtures of [D$_6$]DMSO and H$_2$O at
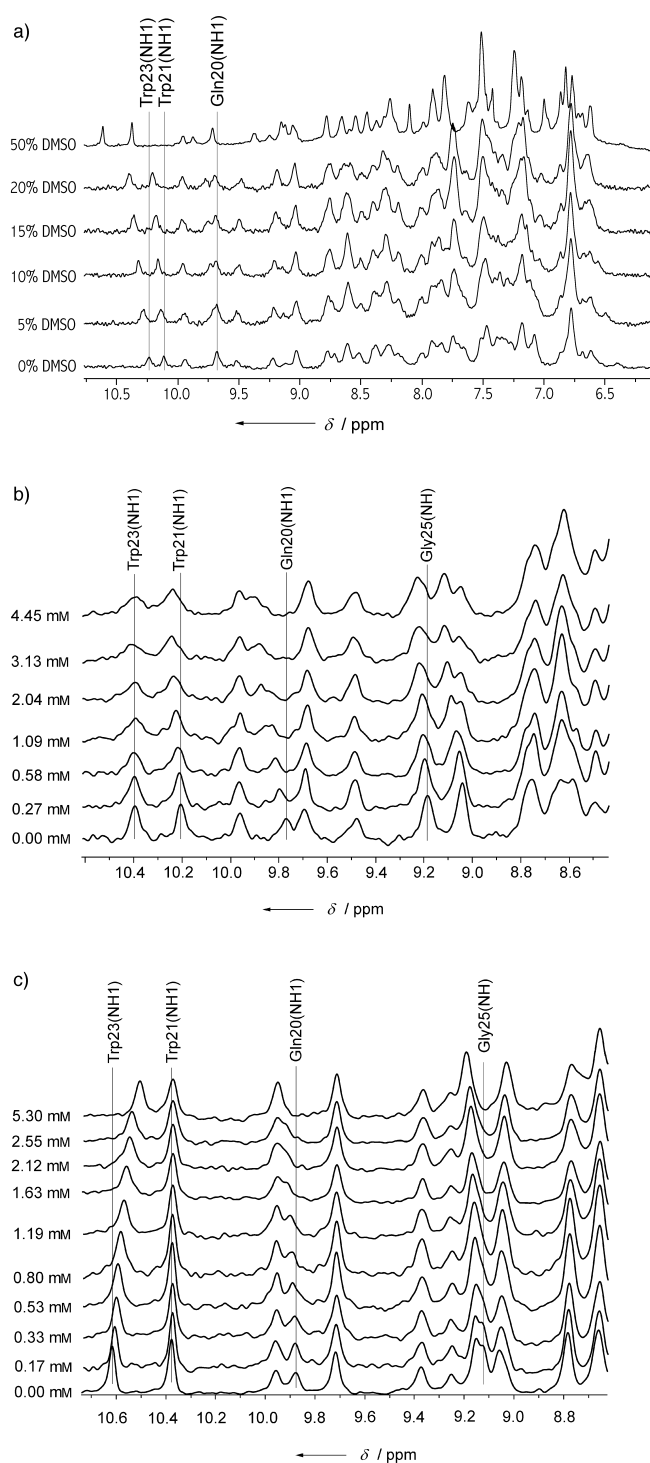

Figure 1. *NMR spectroscopic study of hevein in DMSO/water mixtures at different volume ratios of [D$_6$]DMSO/H$_2$O (a) and in the course of a titration yielding different ratios of N,N',N''-triacetylchitotriose/hevein in [D$_6$]DMSO/H$_2$O (20:80, v/v) at T = 305 K, a constant hevein concentration of 0.39 mM, and N,N',N''-triacetylchitotriose concentrations of 0.27, 0.58, 1.09, 2.04, 3.13, or 4.45 mM, respectively (b), and at 50:50 volume ratio at T = 309 K, a constant hevein concentration of 0.3 mM, N,N',N''-triacetylchitotriose concentrations of 0.17, 0.33, 0.53, 0.80, 1.19, 1.63, 2.12, 2.55, or 5.30 mM, respectively (c). The volume ratio of DMSO increases from bottom to top. The spectrum at the bottom of the figure is obtained with hevein dissolved in pure water (a). The amount of N,N',N''-triacetylchitotriose increases from bottom to top. The spectrum at the bottom of the figure represents a measurement of hevein without any addition of ligand (b, c).*

volume percentages of either 20:80 or 50:50. In the case of stepwise additions of *N,N′,N′′*-triacetylchitotriose to hevein dissolved in a mixture of 20:80 [D$_6$]DMSO/H$_2$O, a significant increase of line broadening and shifts of signal positions were observed: The signals of the NH protons of Trp 21 and Trp 23 were significantly broadened. However, it is analytically problematic, for example due to signal overlap, to base affinity calculations on this parameter. Thus, we placed emphasis on chemical shifts. The NH1 signal of Trp 21 and Glu 20 as well as the NH signal of Gly 25 moved downfield with increasing *N,N′,N′′*-triacetylchitotriose concentration (Figure 1 b). Also, the signal of the γ proton of Gln 20 altered its position by moving upfield. Binding constant (K_b value) and the free-energy change were calculated from the signal shifts at six ligand concentrations (see Figure 1 b). Since signals of different side chains were affected and monitored, we performed separate calculations with each individual parameter. Overall, the binding affinity in 20 % [D$_6$]DMSO decreased by about one order of magnitude to $K_b \approx$ 1000 M^{-1} relative to the results in water (Table 1). An average ΔG value of -17.3 kJ mol^{-1} is obtained. These experiments underscored that addition of DMSO up to a concentration of 20 % affected binding of the ligand but did not impair the capacity for association completely.

In the next step, the effect of a further increase of the DMSO concentration to 50 % was evaluated. The signals of the NH protons of Gln 20 and Gly 25 continued to be shifted downfield

with increasing *N,N′,N′′*-triacetylchitotriose concentration. The NH1 proton of Trp 23 and the NH proton of Gly 25 showed an upfield shift with stepwise addition of *N,N′,N′′*-triacetylchitotriose to hevein in NMR titration experiments carried out in a mixture of [D$_6$]DMSO/H$_2$O (50:50), while the signal of the NH1 proton of Gln 20 moved downfield. As demonstrated by the NMR spectra of the complex in the solvent mixture (Figure 1 c), ligand-binding capacity was operative for the small lectin molecule even at this volume ratio of the organic solvent. When the titration protocol was performed under these conditions with nine different ligand concentrations, a further substantial decrease of the affinity constant to 506 ± 87 M^{-1} was noted (Table 1). Inspection of the individual enthalpic and entropic contributions delineated a preferential impact on the enthalpic term (data not shown). Viewing the individual sensor resonances separately, the decrease in ΔG was especially pronounced for the NH1 proton of Trp 21 (Table 1). The titration analysis showed that the two side chains of Trp 21 and Trp 23 definitely participated in binding in DMSO/water mixtures.

Discussing the apparent sensitivity of the conformation of this small lectin to environmental changes it is also instructive to refer to the significant differences between its solution structures in water and in dioxane/water on the one hand and the crystal structure derived from crystals grown in the presence of 2-methyl-2,4-pentanediol on the other hand.[40, 42, 46, 47]

Table 1. *Chemical shifts, binding constants (K$_b$) and ΔG values obtained from a NMR titration study of* N,N′,N′′-*triacetylchitotriose with hevein in mixtures of DMSO and water.*

		DMSO/water (20:80, v/v)			
T = 300 K	Trp 21(NH1)	Gln 20(NH1)	Gln 20(γH)	Gly 25(NH)	$\bar{x}$[a]
δ_{free} [ppm]	10.24 ± 0.001	9.879 ± 0.003	0.571 ± 0.005	9.207 ± 0.001	
δ_{bound} [ppm]	10.30 ± 0.002	10.040 ± 0.003	0.303 ± 0.004	9.268 ± 0.001	
K_b [M^{-1}]	394 ± 43	1198 ± 131	1236 ± 119	1368 ± 150	1049 ± 111
ΔG [kJ mol^{-1}]	− 14.9 ± 0.25	− 17.68 ± 0.26	− 17.75 ± 0.25	− 18.01 ± 0.27	− 17.09 ± 0.25
T = 305 K	Trp 21(NH1)	Gln 20(NH1)	Gln 20(γH)	Gly 25(NH)	$\bar{x}$
δ_{free} [ppm]	10.21 ± 0.001	9.775 ± 0.003	0.675 ± 0.006	9.19 ± 0.001	
δ_{bound} [ppm]	10.26 ± 0.001	9.944 ± 0.009	0.349 ± 0.016	9.238 ± 0.003	
K_b [M^{-1}]	917 ± 360	784 ± 143	831 ± 137	1352 ± 360	971 ± 250
ΔG [kJ mol^{-1}]	− 17.29 ± 1.1	− 16.9 ± 0.4	− 17.05 ± 0.4	− 18.28 ± 0.7	− 17.38 ± 0.65
T = 310 K	Trp 21(NH1)	Gln 20(NH1)	Gln 20(γH)	Gly 25(NH)	$\bar{x}$
δ_{free} [ppm]	10.20 ± 0.001	9.819 ± 0.002	0.656 ± 0.003	9.18 ± 0.001	
δ_{bound} [ppm]	10.26 ± 0.001	9.977 ± 0.002	0.356 ± 0.003	9.236 ± 0.001	
K_b [M^{-1}]	636 ± 75	1079 ± 66	911 ± 51	791 ± 30	854 ± 56
ΔG_d [kJ mol^{-1}]	− 16.63 ± 0.31	− 18.0 ± 0.15	− 17.56 ± 0.14	− 17.2 ± 0.1	− 17.35 ± 0.18
T = 315 K	Trp 21(NH1)	Gln 20(NH1)	Gln 20(γH)	Gly 25(NH)	$\bar{x}$
δ_{free} [ppm]	10.18 ± 0.001	9.785 ± 0.003	0.681 ± 0.007	9.169 ± 0.001	
δ_{bound} [ppm]	10.24 ± 0.001	9.957 ± 0.003	0.383 ± 0.008	9.217 ± 0.001	
K_b [M^{-1}]	633 ± 82	762 ± 83	629 ± 81	636 ± 44	665 ± 73
ΔG [kJ mol^{-1}]	− 16.89 ± 0.35	− 17.37 ± 0.31	− 16.87 ± 0.35	− 16.9 ± 0.18	− 17.01 ± 0.3
		DMSO/water (50:50, v/v)			
T = 309 K	Trp 23(NH1)	Gln 20(NH1)	Gly 25(NH)	$\bar{x}$	
δ_{free} [ppm]	10.62 ± 0.001	9.877 ± 0.002	9.129 ± 0.001		
δ_{bound} [ppm]	10.41 ± 0.001	9.967 ± 0.008	9.189 ± 0.003		
K_b [M^{-1}]	231 ± 11	523 ± 131	765 ± 120	506 ± 87	
ΔG [kJ mol^{-1}]	− 14.0 ± 0.1	− 16.1 ± 0.5	− 17.05 ± 0.35	− 15.72 ± 0.3	
[a] $\bar{x}$ = average value.					

Simulation of a hevein – *N,N'*-diacetylchitobiose complex in water and in DMSO

The presented experimental data clearly reveal that ligand binding will be impaired already by the loss of the active structure. Thus, it is experimentally not possible to determine the effect of the solvent on interactions in the course of ligand binding. The only way to infer this influence for this protein is to run computer simulations with a commonly used force field. However, in the case of hevein, for which significant structural changes are detected after solvent exchange, it is not possible to decide whether a solvent effect alone can have an impact on ligand binding (neglecting any changes of the overall conformation). Due to its small size it is possible to address this question by MD simulations of hevein – *N,N'*-diacetylchitobiose complexes. For the MD simulations, hevein was placed in an environment of virtual water or DMSO molecules. To reveal how the interaction with the ligand is affected by the solvent exchange, the essential assumption was made that the overall 3D fold of hevein obtained in water is maintained in DMSO. During the MD simulations in water or DMSO, both GlcNAc residues of the ligand establish contacts with various amino acid residues, although the binding pocket of hevein with Trp 21, Trp 23, Tyr 30, and Ser 19 as key constituents is rather shallow. The complex formation between hevein and the ligand depends on the solvent used in the MD simulation, as graphically shown in Figure 2 a, b. In general, MD simulations with explicit inclusion

Figure 2. *Twenty superimposed snapshots from a MD simulation of the hevein – N,N'-diacetylchitobiose complex in water (a) and DMSO (b). The water or DMSO molecules are not displayed. Only the backbone atoms of the lectin and the side chains of the binding-site amino acids involved in ligand binding are shown in black. In this respect, Ser 19, Trp 21, Trp 23, Glu 29, and Tyr 30 are important constituents of the binding site. The nonreducing residue (GlcNAc') of the ligand N,N'-diacetylchitobiose (GlcNAc'β1-4GlcNAc) is labeled.*

of water molecules confirm the conclusions drawn from the NMR-derived structure[40, 42] (Figure 2 a): The *N*-acetyl group of the nonreducing GlcNAc' residue is located in the binding pocket engaged in nonpolar contacts to Trp 21 and Tyr 30. The orientation of the saccharide rings favors formation of hydrogen

bonds and also stacking interactions with aromatic side chains in water. Together with Ser 19, the three aromatic amino acids Trp 21, Trp 23, and Tyr 30 play a dominant role for the formation of the hevein – *N,N'*-diacetylchitobiose complex.[40–42] As is also evident from Figure 2 a, Trp 21 exhibits a strong stacking interaction with the hydrophobic surface of the reducing GlcNAc moiety. When comparing the results of the MD simulations in the two solvents, it is clear that hydrophobic and stacking interactions significantly contribute to the stability of the complex in water. These contacts are weakened or even completely lost when switching the solvent to DMSO, in which electrostatic contacts are dominant. Thus, the polar character of water molecules favors formation of strong van der Waals contacts between hydrophobic parts of the two molecules. This situation appears to change markedly when using the less polar and partially hydrophobic DMSO as solvent. Polar contacts gain importance leading to a reorientation of several structural features involved in the binding process. As a consequence, only few hydrophobic contacts appear to be maintained. Since the interaction analysis—which can only be used in a qualitative manner—has intimated changes in the binding energy of various segments of the ligand, it is possible to make assumptions despite the given caveats that protein – carbohydrate interactions may not fully be abolished in the aprotic solvent, prompting additional experiments (see below).

In view of the long-range purpose of our study, it is crucial to note that the presence of an aprotic solvent will not necessarily severely harm the activity of the small plant lectin hevein. But the effects of DMSO on hevein's structure and its ligand affinity will hamper further structural analysis of hevein – ligand complexes by using signals from exchangeable hydroxy protons. An inherent drawback is that hevein lacks a compact structural organization, for example characteristic of jelly-roll-motif-harboring proteins with their regular arrangement of β-strands such as galectins. Their activity is known to be resistant to stepwise ethanol and xylene treatment during glycohistochemical processing.[48–50] Considering the remarkable structural stability of various types of sugar receptors, for example, galectins, plant AB toxins, and immunoglobulins, the calculations and the spectra presented in the preceding sections strongly encouraged us to pursue this line of investigation with sugar receptors, whose ligand-binding ability can withstand even a complete solvent change. To explore this new area systematically step by step, we first analyzed the conformational behavior of free ligands in the aprotic solvent. Because MD data are available for them, they are exploited as a source for predictions whether or not new water-sensitive NOE contacts can be expected. With appropriately devised software we systematically screened the array of interproton distances in the course of MD runs for the occurrence of water-sensitive and water-insensitive NOE contacts. The presence of suitable distance constraints involving at least one water-exchangeable proton constitutes an essential prerequisite to prove the applicability of our concept. The next step is to infer receptor activity by using line broadening as a first experimental indication. In principle, it would be convenient to assay this characteristic in a technically simple setting with only a small amount of receptor prior to investing further efforts into
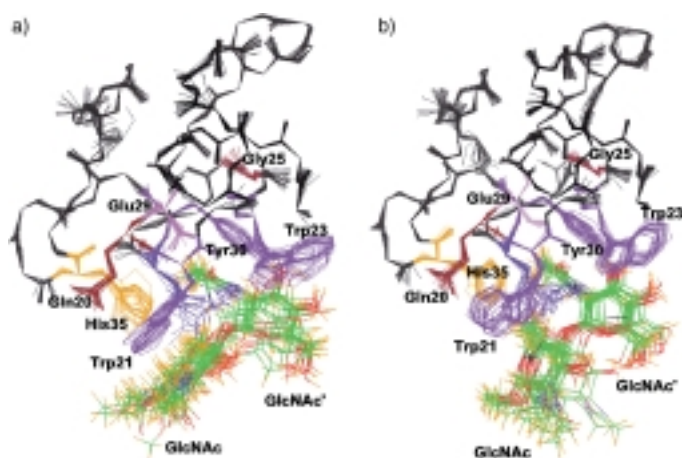
combined computational calculations and NMR spectroscopy. To meet this requirement, we have adapted two types of sensitive solid-phase assays. These biochemical methods enable us to decide whether and to what extent the sugar receptor specifically exhibits binding activity for the presented ligand under such solvent conditions, setting the stage for NMR experiments with protein – carbohydrate complexes in an aprotic solvent.

Conformational analysis of Gal′α1-3Galβ1-R in the free state

The disaccharide Gal′α1-3Galβ1-R interacting avidly with VAA or the purified IgG subfraction has proven to be a suitable model ligand for this study.[51–53] To gain insight into its conformational properties, RAMM calculations at $\varepsilon = 1.5$, 4, and 49 (to mimic DMSO) as well as 80 (to mimic water) and MD simulations with explicit inclusion of solvent molecules were carried out. As shown in Figure 3 a, a central low-energy valley is shaped by the calculations at $\varepsilon = 4$. Remarkably, the damping of the Coulomb term introduced by the stepwise increase of the dielectric constant is already effective at $\varepsilon = 4$, further increases to $\varepsilon = 49$

(DMSO) and $\varepsilon = 80$ (water) exerting no impact on the energy profile (not shown). The RAMM results were flanked independently by the conformational clustering approach (for technical details and information on further digalactosides, see ref. [57]). Five main clusters could be determined, three residing in different area sections within the central energy minimum valley, whereas two clusters were located in the side minimum. Explicitly, the individual parameters for each cluster are as follows:

cluster 1 at $\Phi = -50°$ and $\Psi = -30°$;
cluster 2 at $\Phi = -40°$ and $\Psi = 60°$;
cluster 3 at $\Phi = -10°$ and $\Psi = -30°$;
cluster 4 at $\Phi = -40°$ and $\Psi = -165°$;
cluster 5 at $\Phi = -10°$ and $\Psi = -170°$.

While these calculations depict the local side minimum as potentially populated (clusters 4 and 5), MD simulations on dynamic fluctuations from various starting points will reveal the level of occupancy for each minimum position. The respective MD simulations at room temperature with explicit inclusion of solvent molecules substantiated that molecules will at least preferentially reside in the central energy valley (Figure 3 b). To gain experimental support for the results based on computer-assisted calculations, ROESY spectra were recorded to determine the free-state conformation of this disaccharide in [D$_6$]DMSO (not shown, see Supporting Information). A comparative NOE analysis of the structural aspects of the disaccharides free in solution is feasible in D$_2$O and in [D$_6$]DMSO, following initial work by Casu et al.[28]

The interresidual distances were assessed by using the intensities of the intraresidual proton – proton ROESY cross-signals for calibration, for example, that of Gal H1 and Gal H3 with an intraresidual distance of 2.7 Å. Exploiting this molecular ruler, crosspeak intensities originating in the spectra from through-space contacts of spatially neighboring protons in different sugar units were translated into average distances. In comparison to the number of distance constraints in D$_2$O, three additional OH contacts (Gal′ OH2 ··· Gal OH4, Gal′ H1 ··· Gal OH4, and Gal′ H5 ··· Gal OH2)
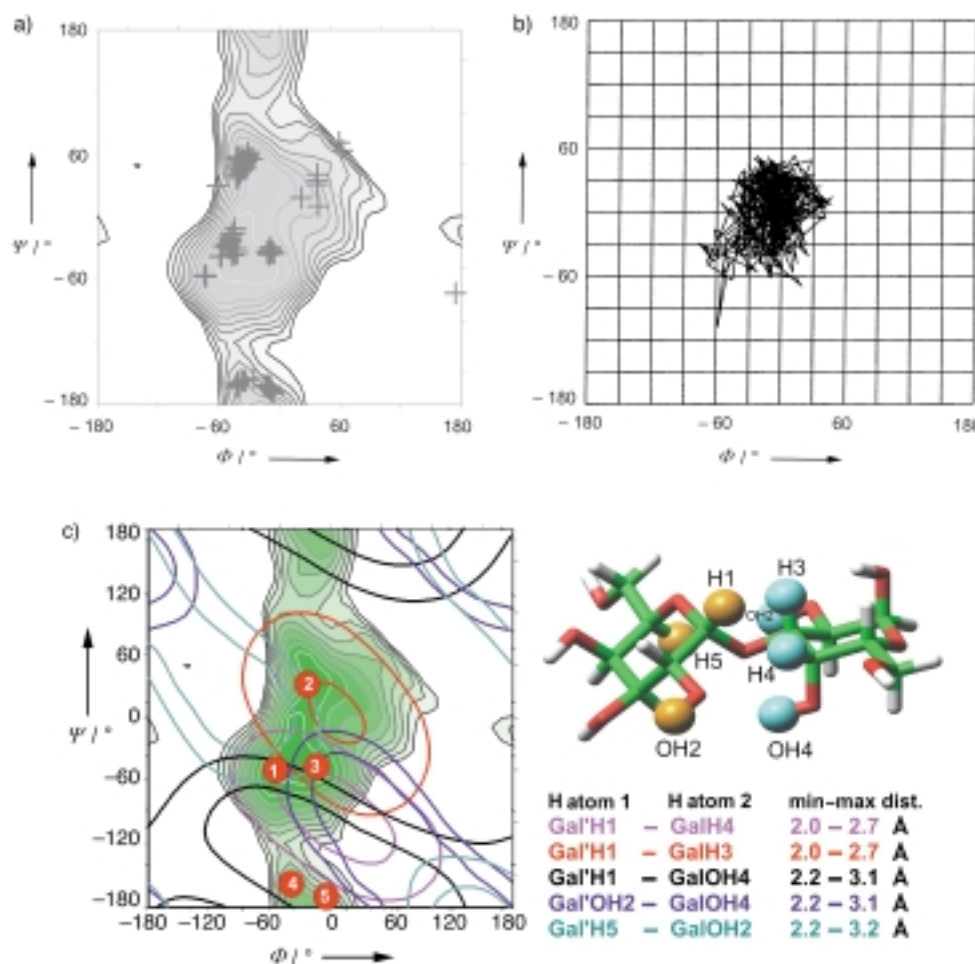

Figure 3. *Energy profile of Gal′α1-3Galβ1-R obtained by RAMM. The crosses refer to individually attained low-energy positions reached from different starting points according to the conformational clustering approach at $\varepsilon = 4$ (a), and representation of the conformational behavior of Gal′α1-3Galβ1-R in a MD simulation using CVFF with explicit inclusion of DMSO molecules (b). c) Distance map obtained from ROESY measurements of Gal′α1-3Galβ1-R (a model is shown on the right) in the free state. Color coding corresponds to the pairs of contour lines.*

H atom 1		H atom 2	min–max dist.
Gal′H1	–	GalH4	2.0 – 2.7 Å
Gal′H1	–	GalH3	2.0 – 2.7 Å
Gal′H1	–	GalOH4	2.2 – 3.1 Å
Gal′OH2	–	GalOH4	2.2 – 3.1 Å
Gal′H5	–	GalOH2	2.2 – 3.2 Å

were recorded in [D_6]DMSO. Not only two, but five pairs of contour lines will thus be available for the definition of the conformational space. The five following interresidual distances lead to this topological characterization:

Gal′ H1 ··· Gal H3 2.7 Å;
Gal′ H1 ··· Gal H4 2.7 Å;
Gal′ H1 ··· Gal OH4 3.1 Å;
Gal′ H5 ··· Gal OH2 3.2 Å;
Gal′ OH2 ··· Gal OH4 2.9 Å.

The corresponding distance map shows two regions of overlap. Their presence may be interpreted to indicate that more than one conformation is detectable in the free state by NMR spectroscopy (Figure 3c). However, only one region of overlap of contour lines lies in an area section distinguished by a low-energy content, as demonstrated by the calculated conformational clusters (compare Figure 3a with Figure 3c). The region of overlap defined by the three interresidual contacts Gal′ H1-··· Gal OH4, Gal′ H5 ··· Gal OH2, and Gal′ OH2 ··· Gal OH4 at $\Phi = 120°$ and $\Psi = 120°$ is very likely artificial due to its unfavorable energy value as shown in Figures 3a and b. Concerning the energy level in the small region of overlap defined by the interresidual contacts Gal′ H1 ··· Gal H3, Gal′ H1 ··· Gal H4, and Gal′ OH2 ··· Gal OH4 its convergence with cluster 3 is intriguing. In fact, the two interresidual contacts Gal′ H1 ··· Gal OH4 and Gal′ H5 ··· Gal OH2 also share conformational space with this region of overlap, nearly merging it to a point. Figure 3c graphically illustrates to what remarkable extent the area of overlap between the contour line pairs of the water-insensitive protons is delimited by the three additional contacts detectable in the aprotic solvent. The combined NOE and MD data are in line with the reasoning that the conformation can apparently switch between different Φ,Ψ sections within the central low-energy valley, which can hardly be distinguished by MD simulations alone (Figure 3b). If any of these contacts showed up in the analysis of complexes by measuring tr-NOEs, the aim of our study, as defined in the Introduction, would be attained. The fact that the two contacts Gal′ H1 ··· Gal H3 (2.7 Å) and Gal′ H1 ··· Gal H4 (2.7 Å) are also measurable in D$_2$O underscores the absence of a major structural distortion imposed by the solvent exchange, as to be expected from the results of the computations.

Having documented with this example that water-exchangeable protons of a ligand for sugar receptors with compact secondary structure can produce NOE signals in DMSO, it was of interest to devise a general method to predict which and how many contacts can be expected to be measurable on the basis of the MD simulation. This computational protocol could favorably reduce the amount of experimental work by enabling to focus efforts on these cases, in which solvent-sensitive contacts in energetically preferred conformations can occur. The results of such a detailed conformational analysis (obtained with the program CAT)[83], using Gal′ H1 or Gal′ OH2 as contact partners from the nonreducing sugar moiety, are shown in Figure 4. When the population density of distances between interresidual protons (C—H as well as O—H protons) was drawn, the

Gal′ OH2 ··· Gal OH4 contact and the Gal′ OH2 ··· Gal H4 contact in Galα1-3Galβ1-R could lead to an interresidual NOE crosspeak (Figure 4a). However, only the Gal′ OH2 ··· Gal OH4 distance constraint was detectable with NOE spectroscopy. This is a contradiction between experimental detection and theoretical simulation since both contacts have nearly the same population profile (Figure 4a). To address this issue the Gal′ OH2 ··· Gal OH4 contact was analyzed during two MD simulations under explicit consideration of the DMSO molecules and in vacuum at a simulation temperature of 300 K (bottom and top of Figure 4b, respectively). If the presence of solvent had no influence on contact distance, no difference would be visible. Figure 4b clearly demonstrates that the distances between Gal′ OH2 and Gal OH4 are affected by the solvent. (A detailed snapshot of an MD simulation can be found in the Supporting Information.) To further illustrate the predictive power of this technique, we have also performed this computation of interproton distance sampling derived from MD runs for Gal′β1-3Galβ1-R (Figure 4c). In the anomeric variant the protons Gal′ OH2 and Gal OH4 were separated by more than 4 Å when reaching the maximum level of population density. In agreement with this finding, the respective signals were not visible in the ROESY spectrum (not shown). Only the expected Gal′ H1 ··· Gal OH2 contact could be observed in [D_6]DMSO (not shown, see Supporting Information).

The actual possibility to gain access to an OH-group-dependent signal of the free ligand encouraged us to carry out further NMR experiments in the presence of a receptor. By addition of two disaccharides with known affinity for the chosen lectins and IgG, we analyzed the impact of the receptor on the OH signals of the ligand as a first indication for complex formation.

Line-broadening effects of ligand hydroxy groups in carbohydrate – protein complexes in pure DMSO solution

The proton signals of the OH groups of Gal′α1-3Galβ1-R and Gal′β1-2Galβ1-R were assigned by COSY, TOCSY, and ROESY experiments. Addition of a sugar receptor completed the system for further analysis of the signals of the disaccharides. Significant line broadening and ppm shifts were monitored in pure [D_6]DMSO for Gal′α1-3Galβ1-R complexed with VAA and for the same disaccharide bound to the α-galactoside-binding IgG subfraction from human serum (Figure 5a, b). Responses indicative of binding in the aprotic solvent could also be detected for the synthetic high-affinity ligand Gal′β1-2Galβ1-R in the presence of VAA or in the presence of the galectin from chicken liver (CG-16) (see Supporting Information), which has marked structural homology to mammalian galectin-1.[54] Characteristic indications for line broadening (e.g., for the 3′-OH group of the Gal residue at the reducing end) were observed. Identical results were obtained when galectin-1 from bovine heart was used instead of CG-16 underscoring the close similarity in their folding patterns (data not shown). Since legume lectins also share the jelly roll motif,[55] it is likely that they can also be included in this type of analysis. The alterations of the half-width of proton signals from OH groups served as an indication for complex formation, as seen above for the signals of hevein which were broadened after ligand addition in [D_6]DMSO/D$_2$O mixture.
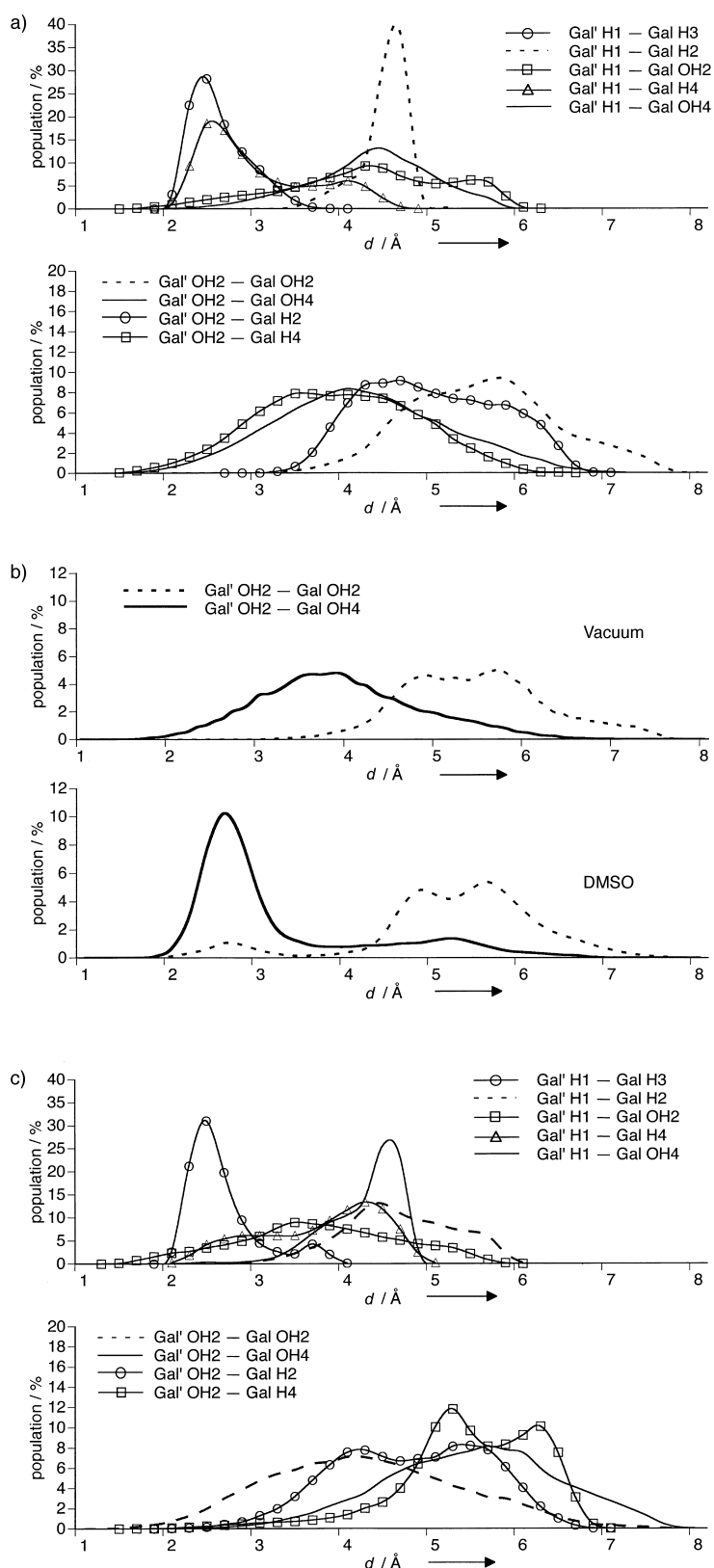
a)

b)

c)

Figure 4. *Calculated frequency profiles for interresidual proton distances (CH⋯CH, CH⋯OH, and OH⋯OH proton pairs with involvement of Gal′ H1 and Gal′ OH2). Population percentages are derived from the frequency of the occurrence of a given distance during the MD simulation for Gal′α1-3Galβ1-R at T = 400 K (a), Gal′α1-3Galβ1-R at T = 300 K (b), and Gal′β1-3Galβ1-R at T = 400 K (c). MD simulations were carried out in the gas phase (vacuum) (a; b, top; c) or with explicit consideration of DMSO molecules (b, bottom).*

Responsibility for an increase in line width can be ascribed to unspecific interactions, exchange effects, and the enhanced viscosity. Such effects yet normally influence this parameter in all signals. This was not the case in our measurements. For example, the OH-2 and OH-6 proton signals of Gal′ (the monosaccharide unit at the nonreducing end) were affected most strongly in comparison to the other protons of Gal′α1-3Galβ1-R, especially when complexed with VAA (Figure 5a). To prove the implied specific sugar – protein interaction with an independent biochemical method, solid-phase ligand-binding assays were carried out. They have an additional advantage as screening tools, because only a small amount of substance (microgram range) is required.

Solid-phase ligand-binding assays

An essential prerequisite to be fulfilled for measuring additional solvent-sensitive tr-NOE signals in receptor – ligand mixtures is that the sugar receptors retain their capacity for specific ligand recognition in the aprotic organic solvent. To verify this assumption beads of the affinity resin bearing covalently immobilized disaccharides (lactose, melibiose) were employed in a solid-phase assay for the plant lectin VAA, bovine galectin-1, and the affinity-purified IgG subfraction. The assays in the two solvents were carried out in parallel with aliquots from the same protein stock solution to avoid any influence of batch variation. As given in detail in the Experimental Section, the proteins had been invariably dissolved in aqueous stock solution which was subsequently diluted in a large excess of assay solvent. This processing ensured precise protein quantities to be obtained even in the aprotic solvent, but it necessarily led to the presence of minute amounts of water (i.e., below 5 µL H_2O per mL of DMSO in the first assay and up to 10 µL H_2O per mL of DMSO in the second assay; for practical details, see Experimental Section). To enable a direct comparison of the extent of specific binding in the two solvent systems for each type of sugar receptor, not the total binding but the extent of sugar-inhibitable (specific) binding is illustrated. Evidently, the tested sugar receptors can bind to the exposed disaccharides in the organic solvent, albeit with quantitative variations (Figure 6). The extent of sugar-inhibitable binding was substantially reduced in DMSO for the immunoglobulin G subfraction and the plant lectin, while the reduction was rather small for the galectin. In contrast to hevein, these sugar receptors were still active in DMSO, warranting further characterization of their binding behavior. These positive assay results also confirmed the validity of the assumption for specific binding as the reason for line broadening described in the preceding section, and the value of the method as a screening tool.
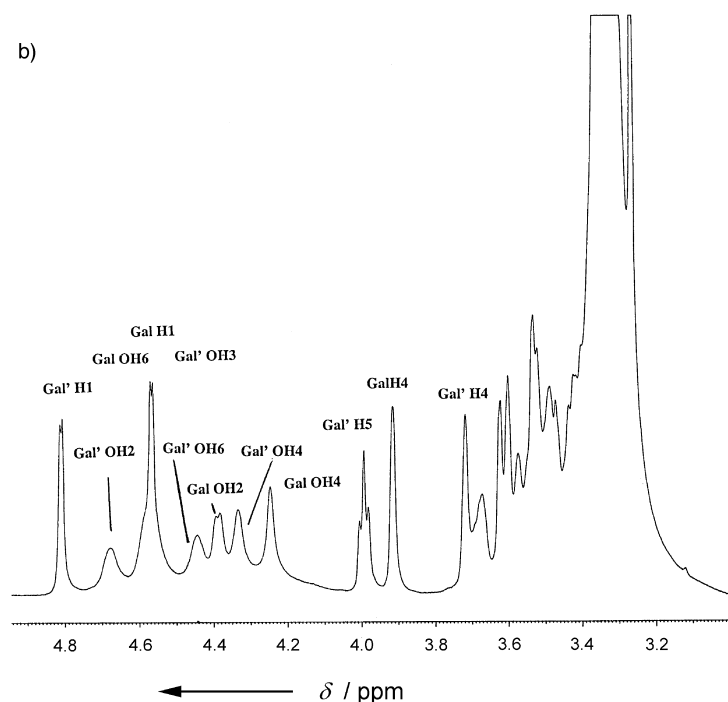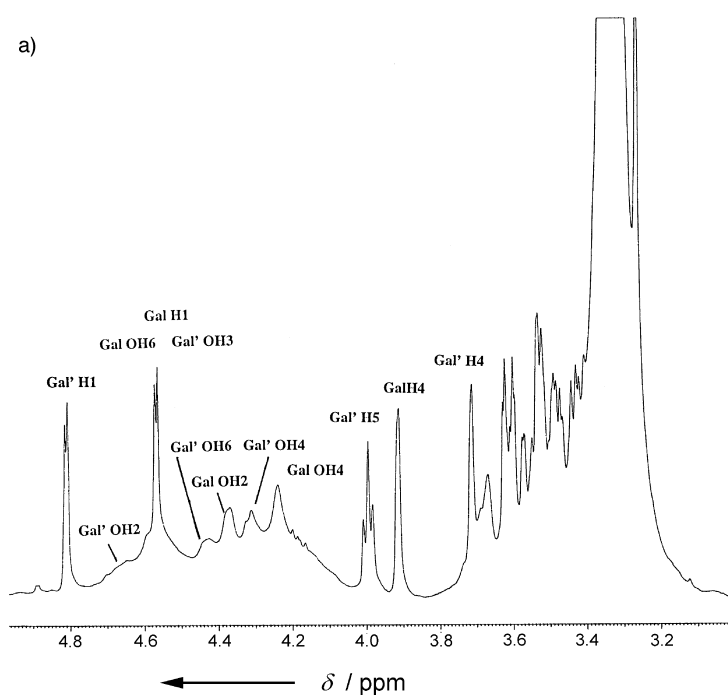
a)

b)

Figure 5. *1D NMR spectrum of Gal'α1-3Galβ1-R in [D₆]DMSO complexed with VAA (a) or with the α-galactoside-binding IgG subfraction (b). In both cases, a tenfold molar excess of the ligand was used.*
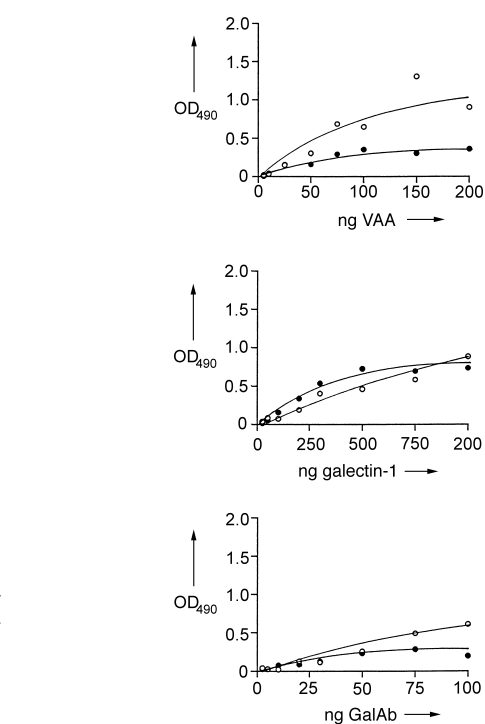

Figure 6. *Illustration of the extent of sugar-inhibitable binding of labeled VAA (top), galectin-1 (middle), and the α-galactoside-binding IgG subfraction (GalAb, bottom) to carbohydrate-ligand-exposing Sepharose beads in aqueous solution (○) and the aprotic solvent (●).*
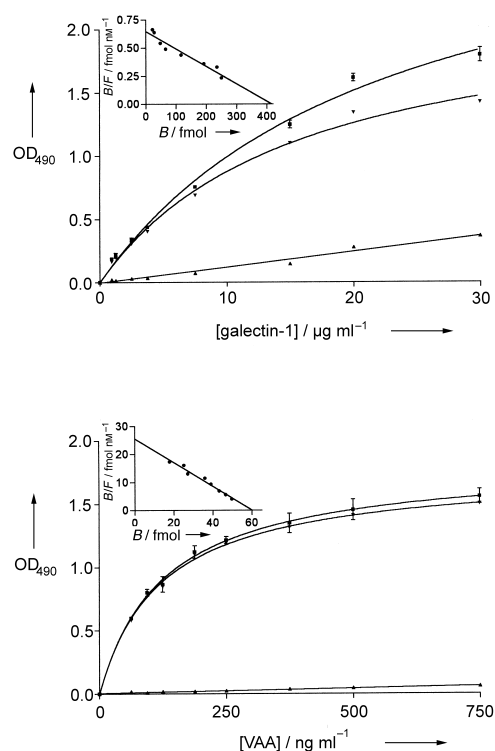

Figure 7. *Determination of sugar-inhibitable binding (▼) of labeled galectin-1 (top) and VAA (bottom) to surface-immobilized ligand in aprotic solvent. The insets show Scatchard analyses of the binding data (see also Table 2). Total binding (■) was reduced by the extent of noninhibitable binding (▲) to exclude any sugar-independent contributions from the calculations. B = quantity of bound lectin molecules; F = concentration of free lectin.*

Comparative quantitation of thermodynamic parameters of binding was achieved by Scatchard plot analysis of data for binding to surface-immobilized ligands, as exemplarily documented in Figure 7. Rather minor alterations in K_D and B_{max} values were measured for immunoglobulin G with its compact and remarkably stable Ig fold of the antigen-binding site (Table 2). K_D value and extent of binding were significantly decreased ($p =$ 0.031, 0.014) for the plant lectin. The threshold of 0.05 for

Table 2. *Scatchard analysis of the effect of solvent on the binding of three galactoside-specific proteins to (neo)glycoconjugates in a solid-phase assay.*[a]

Solvent	Receptor		
	VAA	Galectin-1	α-Gal-IgG
PBS	$B_{max} = (8.49 \pm 1.93) \times 10^{10}$	$B_{max} = (0.79 \pm 0.44) \times 10^{10}$	$B_{max} = (1.62 \pm 0.56) \times 10^{10}$
PBS	$K_D = (6.57 \pm 3.53) \times 10^{-8}$	$K_D = (1.29 \pm 0.26) \times 10^{-6}$	$K_D = (8.14 \pm 3.59) \times 10^{-9}$
DMSO	$B_{max} = (3.89 \pm 0.14) \times 10^{10}$	$B_{max} = (1.90 \pm 0.53) \times 10^{11}$	$B_{max} = (1.55 \pm 0.79) \times 10^{10}$
DMSO	$K_D = (0.34 \pm 0.14) \times 10^{-8}$	$K_D = (0.52 \pm 0.16) \times 10^{-6}$	$K_D = (4.14 \pm 2.55) \times 10^{-9}$

[a] Mean values $\pm$ standard deviation are given on the basis of at least three individual experiments. For the different sugar receptors, the optimal glycoligand was immobilized on the surface of the microtiter plate wells (PL-Lac for VAA, ASF for galectin-1, and PL-Mel for α-Gal-IgG). B_{max} refers to the apparent number of bound probe molecules per well at saturational concentration of a receptor (1 mg coated ligand). The dissociation constant K_D is given in M.

significance was also passed in the case of the affinity decrease with galectin-1 ($p = 0.017$). When comparing the results of the van't Hoff analysis for hevein with these data obtained in nearly water-free DMSO, it is evident that the small plant lectin's binding capacity is considerably more sensitive to the presence of DMSO than that of any of the three other sugar receptors tested. Both assay types corroborate each other in revealing that sensitive detection methods can pick up activity in the aprotic solvent. Specificity controls excluded the possibility that non-specific interactions can account for this measured binding, also allaying concerns voiced in the context of discussing the line broadening. Such a contribution was observed for binding of glycolipids and glycolipid-derived oligosaccharides to a snail lectin (*Helix pomatia* agglutinin) in 50 – 95 % tetrahydrofuran.[56] Since our results independently confirmed the validity of the indispensable prerequisite that at least some sugar receptors can retain capacity for specific ligand recognition in an organic solvent, the issue could be addressed whether the envisioned advantages of tr-NOE measurements on protein – carbohydrate interactions in DMSO will indeed be effective.

NOESY measurements of Gal'β1-2Galβ1-R –, Gal'β1-3Galβ1-R –, and Gal'α1-3Galβ1-R – protein complexes in pure [D$_6$]DMSO and in mixtures of [D$_6$]DMSO and D$_2$O

Based on the rather minor alterations in binding characteristics between the two solvents (Table 2), NMR experiments were

started with the α-galactoside-binding IgG subfraction. Indeed, negative NOE signals indicative of binding could be found, and a water-sensitive third contact was detectable under these conditions (Figure 8 a). In the same way as carried out for the free state, the intraresidual distances were chosen for calibration of the NOE intensities. For Gal'α1-3Galβ1-R the following three interresidual distances were calculated on the basis of the signal intensities of two-spin interactions in the 2D tr-NOE spectrum: Gal' H1 ··· Gal H3 (2.7 Å), Gal' H1 ··· Gal H4 (2.7 Å), and Gal' OH2 ··· Gal OH4 (2.8 Å). A major reason for concern in the interpretation of tr-NOE spectra is the possibility of spin diffusion and rapid proton exchange of OH groups concealing important information for the conformational analysis. To avoid being misled by three-spin processes the mixing time was systematically varied and experimental series were also performed in the rotating frame (tr-ROE experiments).[57, 58] Since interpretations of measurements in DMSO inevitably face the same problems, as can be seen in Figure 8 b, it was important to exploit the recently developed and validated approach with aluminum oxide as suppressor of proton exchange.[59] Al$_2$O$_3$ is a strongly hygroscopic substance, which also acts as a proton acceptor blocking the magnetization transfer between protons from OH groups and those of the environment. Up to 10 mg of this substance per NMR assay sample (0.4 mL of solvent) reduced proton exchange processes in the case of the α-galactoside-binding IgG subfraction. Only the genuine OH ··· OH contact remained in the spectrum, as demonstrated by the comparison between Figures 8 a and b.
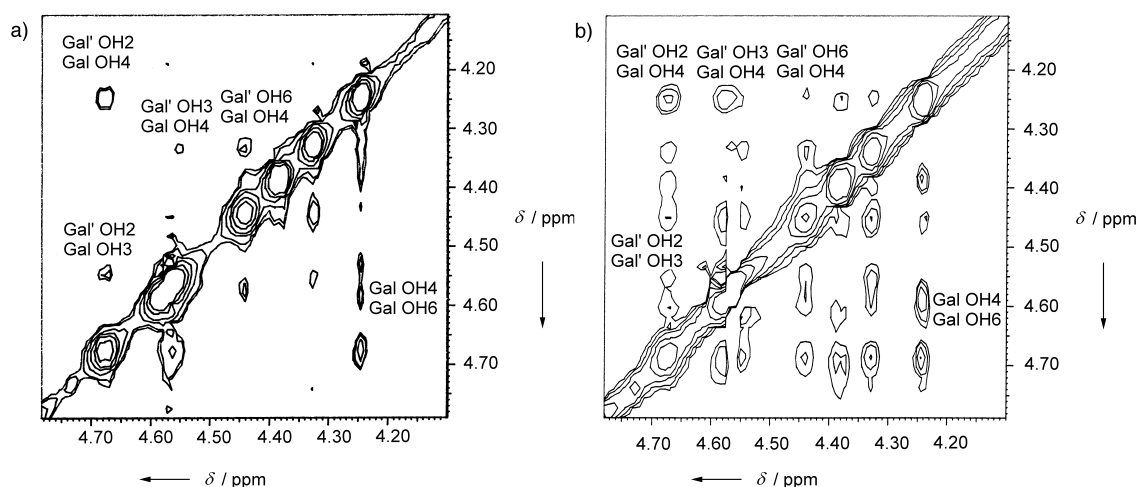

Figure 8. *Relevant part of a 2D tr-NOE spectrum (mixing time 80 ms) of the Gal'α1-3Galβ1-R – antibody complex in the presence (a) and the absence of Al$_2$O$_3$ (b).*
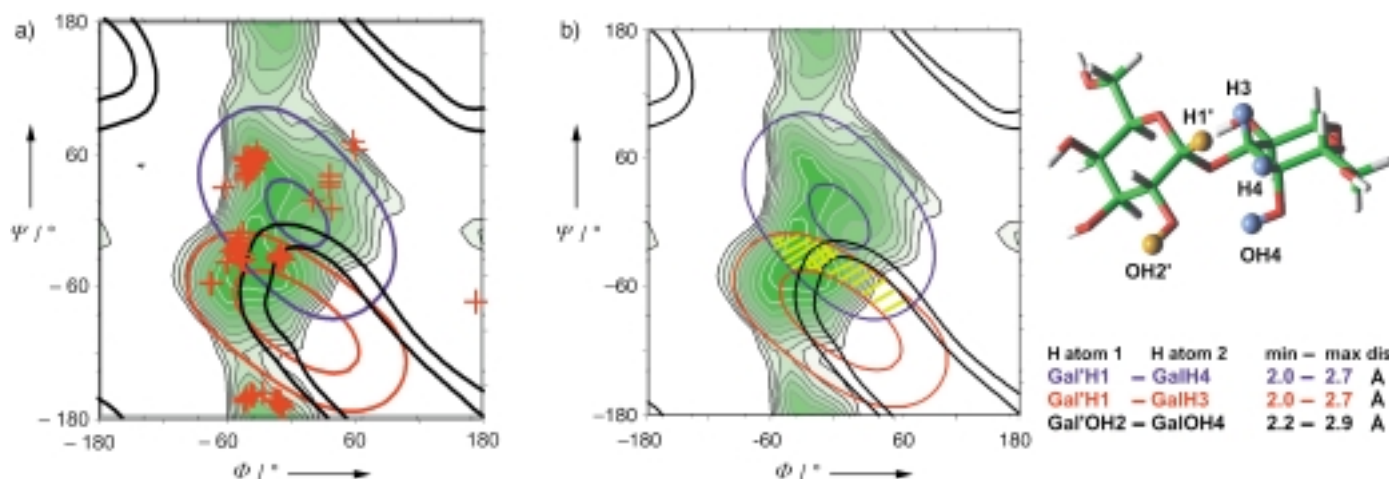
Figure 9. *Introduction of the experimentally determined conformational constraints based on the two water-insensitive and the additional water-sensitive interresidual NOE contacts of Gal'α1-3Galβ1-R into the Φ,Ψ,E-plot. The area of overlap between the contour line pairs from the two water-insensitive contacts lies in the central low-energy valley, also encircling crosses derived from the RAMM procedure (a), and the size reduction of the allowed conformational area by the third water-sensitive contact is highlighted (b). The color coding corresponds to the pairs of contour lines.*

On the basis of the Gal' H1 ··· Gal H3, the Gal' H1 ··· Gal H4, and the Gal' OH2 ··· Gal OH4 contacts the conformational analysis of antibody-bound Gal'α1-3Galβ1-R was carried out to evaluate the extent of information provided by the solvent-sensitive third contact. The two interresidual contacts Gal' H1 ··· Gal OH4 and Gal' H5 ··· Gal OH2 of the free state were not registered. Picking up the thread of interpretation of the NOE signals of the free state, it is reasonable to assume a restriction of mobility in the central low-energy valley by formation of the ligand–receptor complex. As performed with the information on the contacts of the free ligand, the three interresidual signals were translated into pairs of contour lines of the distance map (Figure 9a, b). Since the third pair of contour lines shared an area of overlap with those of the solvent-insensitive signals, the definition of the conformational space of the bound ligand, highlighted in Figure 9a, b, has become considerably more refined. Fittingly, the defined area of overlap is congruent with pairs of Φ,Ψ-values that are adopted during the MD simulations of this disaccharide in the free state (Figure 3b). When comparing Figure 3a with Figure 9a, b, it is satisfying to see that cluster 3 is exactly located in the area section of overlap defined by the three experimentally derived contour line pairs. In case a conformation in accordance with cluster 1 would be adopted in the bound state, we should have been able to detect contact Gal' H5 ··· Gal OH2. Therefore, our results provide an example of conformer selection, previously seen for lectins,[13, 20, 57, 60] in the case of an immunoglobulin subfraction from human serum. Furthermore, it was possible for the first time to use a proton signal of an OH group of a bound ligand in an aprotic solvent to refine the description of the topology of the sugar-receptor-bound state of a disaccharide.

Additional tr-NOE experiments with the plant lectin VAA and with galectins (galectin-1, CG-16) confirmed that this result is by no means exceptional (data not shown). They also underscore the importance of the combination of the biochemical assays with the computational screening to focus efforts on promising receptor–ligand pairs.

In this context, one further issue warrants to be addressed. Under the given conditions, the described approach is readily applicable to sugar receptors, whose activity can withstand a (nearly) complete solvent exchange. Considering the demonstrated sensitivity of hevein, it is tempting to modify the basic procedure in order to accommodate even carbohydrate-binding proteins for which the pure aprotic solvent can be harmful. In case the proton exchange can be reduced by the presence of the aprotic solvent in a mixture with water at decreased temperature, a route could be opened for experiments with a wide range of receptor proteins due to lifting the restrictive conditions of a complete solvent exchange. To establish an assay system for the tedious attempts towards this aim, we have focused on the plant lectin VAA.

Intra- and interresidual tr-NOE signals were measured for Gal'β1-3Galβ1-R – VAA and Gal'α1-3Galβ1-R – VAA complexes in mixtures of 40:60 and 50:50 [D_6]DMSO:D_2O. The tr-NOESY spectra of Gal'α1-3Galβ1-R – VAA complexes obtained in 40:60 [D_6]DMSO:D_2O (Figure 10) presented two key tr-NOE values, Gal' H1 ··· Gal H3 (2.7 Å) and Gal' H1 ··· Gal H4 (2.7 Å). These interresidual NOE signal intensities had also been measured for Gal'α1-3Galβ1-R complexed with the IgG subfraction in pure DMSO and translated into two contour line pairs in the respective distance map (Figure 9). Although a water-sensitive signal was not (yet) detectable, this result already intimates that bound-state conformations of a disaccharide in complex with a distinct receptor under different solvent conditions can at least be very similar. To exclude that this behavior is connected to special properties of a distinct ligand, the anomeric variant has likewise been applied regarding tr-NOE signals in a mixture (Figure 11). Further work is in progress to define physical parameters at the given volume ratio, which allow to measure solvent-sensitive contacts.
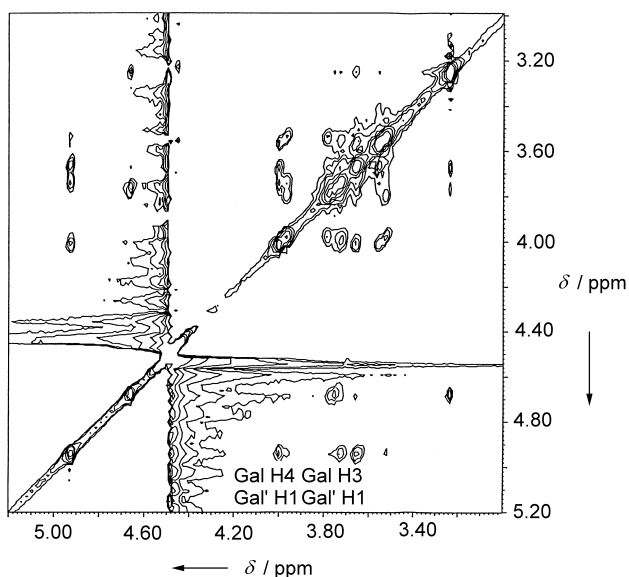
Figure 10. *2D tr-NOESY spectrum (mixing time 200 ms) of Gal'α1-3Galβ1-R complexed with the mistletoe lectin in deuterated [D₆]DMSO/water mixtures (40:60, v/v). A tenfold molar excess of the ligand was used.*
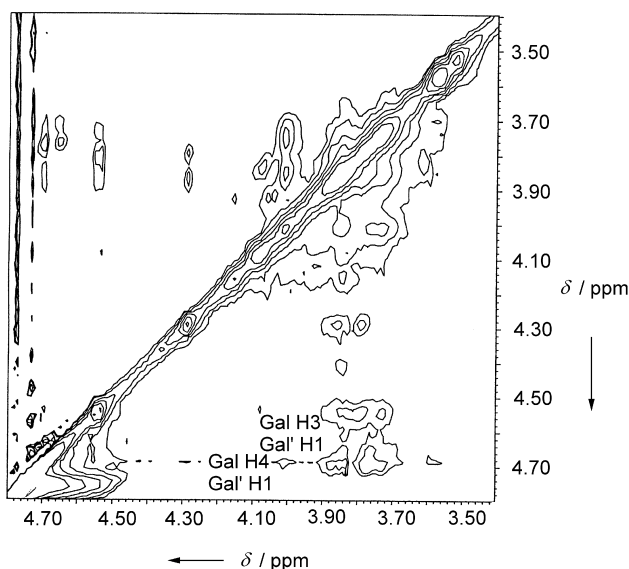

Figure 11. *2D tr-NOESY spectrum (mixing time 200 ms) of Gal'β1-3Galβ1-R complexed with the mistletoe lectin in deuterated [D₆]DMSO/water mixtures (40:60, v/v). A tenfold molar excess of the ligand was used.*

Conclusion

A nonnegligible role in molecular association is attributed to the solvent. Hydrophobic forces and/or enthalpic contributions can critically depend on the degree of order of the water structure at the surfaces of reactants, which impose constraints to yield anisotropic arrangements, and in the bulk solvent. Changes in this parameter are expected to provide clues to understand mechanistic details of complex formation. Already isotopic substitution to D_2O lessens the enthalpic contribution of mono- to trisaccharide binding to concanavalin A by 2.09 –

3.75 kJ mol⁻¹.[61] With solvent reorganization being controversially discussed as a factor contributing to drive ligand association,[12, 62] the documented consideration of an aprotic medium as solvent will aid to delineate the role of these small molecules beyond being passive bystanders. Assessments of thermodynamic parameters in the aprotic solvent or in mixtures, extending previous measurements for the plant lectin and the chicken galectin in water[63] which were also tested in our study, and of conformational constraints from water-exchangeable proton(s) appear to be practicable. For this route of analysis, which is promising not only in lectin research, it is reassuring to note that the tested digalactosides most probably bind with the same topology to their receptors when dissolved in DMSO and in D_2O. The concern of total abolishment of binding capacity by solvent exchange could be allayed not only for the small lectin hevein. Compact folding patterns of β-strands embedding the carbohydrate recognition domain are rather conducive to limiting the activity loss. The affinity of the interaction of the galactoside-binding receptors with carbohydrate ligands was ascertained to be reduced, but not abolished at all. Interestingly, even the loss of tertiary structural elements by solvent exposure will not necessarily eliminate the ligand-binding capacity, as also documented for the peanut agglutinin that had been transformed to a molten-globule-like state by treatment with 1.8 M guanidine hydrochloride.[64]

With respect to NMR analysis of the bound ligand, prior activity assays after solvent exchange and the inspection of interproton distance profiles in MD calculations will set the stage to screen tr-NOE spectra for additional information from water-exchangeable protons of hydroxy groups, provided that the compact folding pattern in and around the carbohydrate recognition domain is maintained and electrostatic repulsion does not become detrimental.

Herein, we document for the first time the measurement of an OH-group-dependent contact of a bound ligand in DMSO as solvent. Since DMSO has little proton-donating capacity, sugar receptors requiring water molecules as mediators with donor potential in the binding site, for example legume lectins or bacterial serogroup-antigen-specific antibodies,[55, 65, 66] can only be subjected to this type of analysis successfully if these crucial solvent molecule(s) is (are) bound tightly. How a lectin responds to displacements of the water molecules initially residing in the binding site as substitutes for the ligand (six in the case of chicken galectin CG-16)[54] after accommodation of the sugar is one of the intriguing questions prompted by our experiments. Having proven that this approach is practically useful, work in this field can now be systematically extended to identify those solvents with minimal impact on structural features. This can be of general interest in the field of rational drug design. Actually, it could be especially useful when interactions of lipophilic ligands with their receptors are to be studied. Also, the indicated search for optimal monitoring conditions of complexes in mixtures warrants more efforts. Further analytical work pursuing the route of our initial study is expected to profit from the possibility of increasing the number of distance constraints for ligands bound to receptors that retain their active-site topology in the given aprotic solvent.

Experimental Section

Reagents and sugar receptors: Covalent coupling of disaccharides (lactose or melibiose) to Sepharose 4B (Pharmacia, Freiburg, Germany) was performed by divinyl sulfone activation, and the ligand-bearing affinity resins were employed for purification of the galactoside-specific lectin from mistletoe (VAA), bovine heart galectin-1, the chicken galectin from adult liver (CG-16), and a polyclonal immunoglobulin G (IgG, 180 kDa) subfraction from human serum with selectivity for α-galactosides.[51, 67–70] Labeling was carried out with the N-hydroxysuccinimide ester derivative of biotin and biotinamidocaproyl hydrazide (Sigma, Munich, Germany) under activity-preserving conditions as described previously.[51, 52, 71–73] Glycosylated poly-L-lysine was prepared by reductive amination with $NaCNBH_3$ as described previously.[69] Hevein was purified as described previously,[41] and its ligands were purchased from Sigma. The disaccharides Gal'α1-3Galβ1-R, Gal'β1-2Galβ1-R, and Gal'β1-3Galβ1-R were synthesized as previously described in detail.[53, 60] The Gal residue of the nonreducing end is denoted as Gal' in order to distinguish it from the Gal residue at the reducing (derivatized) end. A corresponding notation was used for N,N'-diacetylchitobiose (GlcNAc'β1-4GlcNAc).

MD simulations in water or DMSO and RAMM calculations at different dielectric constants: The analysis of the conformational behavior of hevein[40–42] and the disaccharide Gal'α1-3Galβ1-R were mainly based on MD simulations. These were performed with the program DISCOVER 2.95 (MSI, San Diego, CA, USA) on an IBM-SP2 parallel machine applying the consistent-valence force field (CVFF).[74, 75] The input for MD simulations (DISCOVER 2.95) of the disaccharide were designed following the automatic charge and parameter assignment procedure of INSIGHTII 2.5 (MSI). The solvent molecule models of water and of DMSO were explicitly included into the simulation.

For a start conformation in the MD simulations in water or in DMSO, NMR data of a hevein – N,N'-diacetylchitobiose complex in water were used.[40, 42] The automatic assignment of partial charges and atom type according to the applied force field (CVFF) for each atom was accomplished by using the INSIGHTII software. A formal charge of ± 1 was attributed to the polar side chains. The total charge of the protein was -2. The center of gravity of the lectin – ligand complex was placed into a virtual cube with a side length of 35 Å, with periodic boundary conditions and a cutoff limit from 9 to 11 Å (see DISCOVER manual, May **1994**, pp. 2 – 14). For the MD calculations in DMSO, we applied the simulation approach described in refs. [76, 77] To enable MD runs in an environment equivalent to that in the measurements, the virtual cube was filled with solvent molecules. The density difference between the two solvents ($d_{DMSO} = 1.1$ g mL^{-1}, $d_{H_2O} = 1$ g mL^{-1} at 293 K) was accounted for in the simulations. In both cases the α-carbon atoms were fixed to avoid spatial fluctuations. Each molecular ensemble was subjected to an MD simulation for a period of 1000 ps. The simulation temperature was set to 300 K. An integration step of 1 fs and storage of a conformation after 500 steps of integration led to 2000 individual conformations from which 10 with the lowest potential energy level were automatically selected and processed for energy minimization of the complete ensemble, using the conjugate-gradient method. An interaction analysis[78] was carried out to evaluate the energetic contributions of certain parts of N,N'-diacetylchitobiose to the process of complexation with hevein.

Furthermore, as an essential part of the evaluation of the binding studies with VAA and IgG, the local energy minima of Gal'α1-3Gal in the Φ,Ψ-plot were located by RAMM calculations at various dielectric constants ($\varepsilon = 1.5, 4, 49,$ or 80) and by the conformational clustering approach at corresponding values for the dielectric constant.[15, 57]

The topological behavior was further evaluated by MD simulations, as recently described for other digalactosides.[57] These MD simulations were the basis for computing the abundance classes of interproton distances for pairs of interresidual protons, including those from hydroxy groups, to determine the theoretical potential for their engagement in an NOE contact.

The "search NOE contact" option of CAT[83] was used to search systematically for all possible NOE contacts occurring during a given MD trajectory. In short, for each conformation analyzed, the distances between various pairs of H atoms are calculated and weighted with $\langle r^{-6} \rangle^{-1/6}$ due to the r^{-6} dependence for NOE values.[81] For each analyzed pair of protons, its population density is printed against the weighted distance enabling a convenient presentation of all possible NOE contacts. A principal prerequisite of this approach is that all relevant conformations are actually populated during simulation and that a conformational equilibrium between the various conformations exists.[84]

NMR spectroscopy and distance mapping: 500 MHz ^{1}H NMR spectra were recorded with Varian Unity 500, Bruker AM and AMX 500 spectrometers at a temperature of 300 K. Titration of hevein dissolved in [D_6]DMSO/H_2O mixtures of different molar ratios with stepwise addition of N,N',N''-triacetylchitotriose was performed following the protocol previously described for hevein in pure water.[40, 42] Different temperatures were used to derive information on enthalpy and entropy of binding based on a van't Hoff analysis. The lyophilized di- and trisaccharides as well as the sugar receptor preparations were dissolved in D_2O or [D_6]DMSO (Merck, Sharp and Dohme, Montreal, Canada) or mixtures of [D_6]DMSO and water. Assignment of the chemical shifts was carried out by standard NMR experiments (COSY, RCT, TOCSY, ROESY). 2D-ROESY measurements were performed to determine the conformations of the disaccharides in the free state. Receptor-bound-state conformations were resolved by 1D- and 2D-tr-NOE experiments. To avoid potential calibration errors, frequency-offset variation and a special spin-lock pulse sequence were applied, as commonly used.[79, 80] ROESY and 1D- and 2D-tr-NOE experiments were carried out at various mixing times ranging from 20 to 200 ms. Al_2O_3 (Merck, Darmstadt, Germany) dried at high temperature (600 K) was used to suppress exchange effects of the OH groups diminishing the exchange constant k so that the condition $k \ll 1/T_1$ is fulfilled.[59]

NOE constraints obtained for the free and the bound states of the carbohydrates were introduced into the distance-mapping procedure to delineate the topology of the ligand.[80, 81] In detail, the Ramachandran-type representation was chosen for the conformational analysis of the glycosidic linkage. The spectroscopically derived distance constraints for each atom pair involved in NOE contacts are denoted by their Φ,Ψ coordinates in the corresponding plots. The Φ,Ψ angles are defined as follows: Φ: H1-C1-O-C2-H2, Ψ: C1-O-C-2-H2. Contour line pairs drawn for lower and upper limits of the possible distances derived from observation of a certain NOE contact still enclose a large number of Φ,Ψ combinations and do not define a distinct conformation. With increasing number of NOE contacts and ensuing reduction of the theoretically accessible conformational area in the plot by overlap of contour line pairs, the number of pairs of Φ,Ψ coordinates is successively delimited.

Solid-phase assays: The binding properties of the plant and animal lectins as well as the human polyclonal immunoglobulin G subfraction with selectivity for α-galactosides were examined in 20 mM phosphate-buffered saline (PBS; pH 7.2) and DMSO in two independent assay systems, using sugar-ligand-bearing Sepharose beads and surface-immobilized (neo)glycoconjugates as sensors. First, 200 mL of suspended gel were carefully washed in PBS by repetitive

cycles of suspension and centrifugation at 3000 rpm, incubated with 500 mL PBS containing 0.1 % (w/v) carbohydrate-free BSA to block any nonspecific protein-binding sites on the beads for 30 min at room temperature, again carefully washed and then either stored in PBS or transferred to DMSO by three cycles of centrifugation and solvent exchange. Packed resin was incubated with a solution of biotinylated sugar receptor in 200 mL solvent, obtained by diluting a sugar-receptor-containing stock solution of either 1 mg galectin-1 or IgG per mL of PBS or 10 mg VAA per μL of PBS in the respective solvent. Using quantities of up to 5 μg VAA, 2 μg galectin-1, and 150 ng IgG per assay, the upper limit for the water content was 10 μL per mL of DMSO for galectin-1, assays with VAA and IgG reaching 2.5 μL per mL and 0.75 μL per mL, respectively. Following an incubation with gentle rotation to effect close contact between beads and the proteins for 60 min at room temperature and six cycles of centrifugation and solvent exchange to remove any unbound probe and residual organic solvent, 200 mL PBS containing 0.1 % BSA and 0.5 mg streptavidin – peroxidase conjugate per mL (Sigma) were added, the mixture was incubated for 30 min at room temperature, residual unbound indicator conjugate was thoroughly removed, and the extent of binding of biotinylated proteins was assessed with *o*-phenylenediamine as chromogenic substrate and spectrophotometric monitoring at 490 nm. Second, a standard solid-phase assay protocol was followed using lactosylated poly-L-lysine as matrix for VAA, asialofetuin for galectin-1, and melibiosylated poly-L-lysine for the human immunoglobulin G subfraction, as described previously.[73] Again, proteins were first dissolved in buffer yielding a concentrated stock solution for further dilutions in the aprotic solvent, thus keeping the water content below 5 μL per mL of solvent. Assessment of the extent of sugar-inhibitable binding was performed in parallel series incubating the labeled probe in the presence of the competitive sugar (0.2 M) in the microtiter plate wells whose surface exposed the ligand.

[1] R. A. Laine in *Glycosciences: Status and Perspectives* (Eds.: H.-J. Gabius, S. Gabius), Chapman & Hall, London, **1997**, pp. 1 – 14.
[2] H.-J. Gabius, *Eur. J. Biochem.* **1997**, *243*, 543 – 576.
[3] H. Kaltner, B. Stierstorfer, *Acta Anat.* **1998**, *161*, 162 – 179.
[4] H. Lis, N. Sharon, *Chem. Rev.* **1998**, *98*, 637 – 674.
[5] A. V. Villalobo, H.-J. Gabius, *Acta Anat.* **1998**, *161*, 110 – 129.
[6] S. André, S. Kojima, N. Yamazaki, C. Fink, H. Kaltner, K. Kayser, H.-J. Gabius, *J. Cancer Res. Clin. Oncol.* **1999**, *125*, 461 – 474.
[7] H.-J. Gabius, K. Kayser, S. Gabius, *Naturwissenschaften* **1995**, *82*, 533 – 543; H.-J. Gabius, *Naturwissenschaften* **2000**, *87*, 108 – 121.
[8] *Curr. Med. Chem.* **1999**, *6*, Issue 2, pp. 92 – 178.
[9] H. Rüdiger, H.-C. Siebert, D. Solís, J. Jiménez-Barbero, A. Romero, C.-W. von der Lieth, T. Diaz-Mauriño, H.-J. Gabius, *Curr. Med. Chem.* **2000**, *7*, 389 – 416.
[10] J. Carver, *Pure Appl. Chem.* **1993**, *65*, 763 – 770.
[11] E. J. Toone, *Curr. Opin. Struct. Biol.* **1994**, *4*, 719 – 728.
[12] R. U. Lemieux, *Acc. Chem. Res.* **1996**, *29*, 373 – 380.
[13] H.-J. Gabius, *Pharmaceut. Res.* **1998**, *15*, 23 – 30.
[14] T. Peters, B. M. Pinto, *Curr. Opin. Struct. Biol.* **1996**, *6*, 710 – 720.
[15] C.-W. von der Lieth, T. Kozár, W. E. Hull, *J. Mol. Struct. (THEOCHEM)* **1996**, *395 – 396*, 225 – 244.
[16] A. Imberty, *Curr. Opin. Struct. Biol.* **1997**, *7*, 617 – 623.
[17] C. A. Bush, M. Martin-Pastor, A. Imberty, *Annu. Rev. Biophys. Biomol. Struct.* **1999**, *28*, 269 – 293.
[18] H.-C. Siebert, C.-W. von der Lieth, M. Gilleron, G. Reuter, J. Wittmann, J. F. G. Vliegenthart, H.-J. Gabius in *Glycosciences: Status and Perspectives* (Eds.: H.-J. Gabius, S. Gabius), Chapman & Hall, London, **1997**, pp. 291 – 310.
[19] A. Poveda, J. Jiménez-Barbero, *Chem. Soc. Rev.* **1998**, *27*, 133 – 143.
[20] C.-W. von der Lieth, H.-C. Siebert, T. Kozár, M. Burchert, M. Frank, M. Gilleron, H. Kaltner, G. Kayser, E. Tajkhorshid, N. V. Bovin, J. F. G. Vliegenthart, H.-J. Gabius, *Acta Anat.* **1998**, *161*, 91 – 109.
[21] J. Jiménez-Barbero, J. L. Asensio, F. J. Cañada, A. Poveda, *Curr. Opin. Struct. Biol.* **1999**, *9*, 549 – 555.
[22] B. R. Leeflang, J. F. G. Vliegenthart, L. M. J. Kroon-Batenburg, B. P. van Eijck, J. Kroon, *Carbohydr. Res.* **1992**, *230*, 41 – 61.
[23] L. Poppe, H. van Halbeek, *J. Am. Chem. Soc.* **1991**, *113*, 363 – 365.
[24] B. R. Leeflang, J. F. G. Vliegenthart, *J. Magn. Reson.* **1990**, *89*, 615 – 619.
[25] B. Adams, L. Lerner, *J. Am. Chem. Soc.* **1992**, *114*, 4827 – 4829.
[26] L. Poppe, H. van Halbeek, *Nat. Struct. Biol.* **1994**, *1*, 215 – 216.
[27] E. W. Sayers, J. L. Weaver, J. H. Prestegaard, *J. Biomol. NMR* **1998**, *12*, 209 – 222.
[28] B. Casu, M. Reggiani, G. G. Gallo, A. Vigevani, *Tetrahedron* **1966**, *22*, 3061 – 3083.
[29] J. Dabrowski, P. Hanfland, H. Egge, U. Dabrowski, *Arch. Biochem. Biophys.* **1981**, *210*, 405 – 411.
[30] Z.-Y. Yan, B. N. N. Rao, C. A. Bush, *J. Am. Chem. Soc.* **1987**, *109*, 7663 – 7669.
[31] S. J. Singer, *Adv. Protein Chem.* **1962**, *17*, 1 – 68.
[32] J. T. Chin, S. L. Wheeler, A. M. Klibanov, *Biotechnol. Bioeng.* **1994**, *44*, 140 – 145.
[33] M. N. Gupta, *Eur. J. Biochem.* **1992**, *203*, 25 – 32.
[34] A. M. Klibanov, *Trends Biotechnol.* **1997**, *15*, 97 – 101.
[35] A. M. Klibanov, *Acc. Chem. Res.* **1990**, *23*, 114 – 120.
[36] M. Jackson, H. H. Mantsch, *Biochim. Biophys. Acta* **1991**, *1078*, 231 – 235.
[37] Y. L. Khmelnitsky, V. V. Mozhaev, A. B. Belova, M. V. Sergeeva, K. Martinek, *Eur. J. Biochem.* **1991**, *198*, 31 – 41.
[38] K. Griebenow, A. M. Klibanov, *J. Am. Chem. Soc.* **1996**, *118*, 11 695 – 11 700.
[39] M. T. Gómez-Puyou, A. Gómez-Puyou, *Crit. Rev. Biochem. Mol. Biol.* **1998**, *33*, 53 – 89.
[40] J. L. Asensio, F. J. Cañada, M. Bruix, A. Rodríguez-Romero, J. Jiménez-Barbero, *Eur. J. Biochem.* **1995**, *230*, 621 – 633.
[41] H.-C. Siebert, C.-W. von der Lieth, R. Kaptein, J. J. Beintema, K. Dijkstra, N. Nuland, U. M. S. Soedjanaatmadja, A. Rice, J. F. G. Vliegenthart, C. S. Wright, H.-J. Gabius, *Proteins* **1997**, *28*, 268 – 284.
[42] J. L. Asensio, F. J. Cañada, M. Bruix, C. Gonzales, N. Khiar, A. Rodríguez-Romero, J. Jiménez-Barbero, *Glycobiology* **1998**, *8*, 569 – 577.
[43] H.-C. Siebert, R. Adar, R. Arango, M. Burchert, H. Kaltner, G. Kayser, E. Tajkhorshid, C.-W. von der Lieth, R. Kaptein, N. Sharon, J. F. G. Vliegenthart, H.-J. Gabius, *Eur. J. Biochem.* **1997**, *249*, 27 – 38.
[44] M. Vijayan, N. Chandra, *Curr. Opin. Struct. Biol.* **1999**, *9*, 707 – 714.
[45] K. Wüthrich, *NMR of Proteins and Nucleic Acids*, Wiley, New York, **1986**.
[46] N. H. Andersen, B. Cao, A. Rodríguez-Romero, B. Arreguin, *Biochemistry* **1993**, *32*, 1407 – 1422.
[47] A. Rodríguez-Romero, K. G. Ravichandran, M. Soriana-Garcia, *FEBS Lett.* **1995**, *291*, 307 – 309.
[48] H.-J. Gabius, S. Gabius, *Adv. Lectin Res.* **1992**, *5*, 123 – 157.
[49] A. Danguy, K. Kayser, N. V. Bovin, H.-J. Gabius, *Trends Glycosci. Glycotechnol.* **1995**, *7*, 261 – 275.

[50] H.-J. Gabius, C. Unverzagt, K. Kayser, *Biotech. Histochem.* **1998**, *73*, 263 – 277.

[51] X. Dong, W. Amselgruber, H. Kaltner, H.-J. Gabius, F. Sinowatz, *Eur. J. Cell Biol.* **1995**, *68*, 96 – 101.

[52] X. Dong, S. André, B. Hofer, K. Kayser, H.-J. Gabius, *Int. J. Oncol.* **1997**, *10*, 709 – 719.

[53] O. E. Galanina, H. Kaltner, L. S. Khraltsova, N. V. Bovin, H.-J. Gabius, *J. Mol. Recognit.* **1997**, *10*, 139 – 147.

[54] P. F. Varela, D. Solís, H. Kaltner, T. Diaz-Mauriño, H.-J. Gabius, A. Romero, *J. Mol. Biol.* **1999**, *294*, 537 – 549.

[55] R. Loris, T. Hamelryck, J. Bouckaert, L. Wyns, *Biochim. Biophys. Acta* **1998**, *1383*, 9 – 36.

[56] D. F. Smith, B. V. Torres, *Methods Enzymol.* **1989**, *179*, 30 – 45.

[57] M. Gilleron, H.-C. Siebert, H. Kaltner, C.-W. von der Lieth, T. Kozár, K. M. Halkes, E. Y. Korchagina, N. V. Bovin, H.-J. Gabius, J. F. G. Vliegenthart, *Eur. J. Biochem.* **1998**, *252*, 416 – 427.

[58] S. R. Arepalli, C. P. J. Glaudemans, G. D. Daves, Jr., P. Kovac, A. Bax, *J. Magn. Reson. B* **1995**, *106*, 195 – 198.

[59] J. Dabrowski, H. Grosskurth, C. Baust, N. E. Nifant'ev, *J. Biomol. NMR* **1998**, *12*, 5534 – 5539.

[60] H.-C. Siebert, M. Gilleron, H. Kaltner, C.-W. von der Lieth, T. Kozár, N. V. Bovin, E. Y. Korchagina, J. F. G. Vliegenthart, H.-J. Gabius, *Biochem. Biophys. Res. Commun.* **1996**, *219*, 205 – 212.

[61] M. C. Chervenak, E. J. Toone, *J. Am. Chem. Soc.* **1994**, *116*, 10533 – 10539.

[62] E. García-Hernández, A. Hernández-Arana, *Protein Sci.* **1999**, *8*, 1075 – 1086.

[63] S. Bharadwaj, H. Kaltner, E. Y. Korchagina, N. V. Bovin, H.-J. Gabius, A. Surolia, *Biochim. Biophys. Acta* **1999**, *1472*, 191 – 196.

[64] G. B. Reddy, V. R. Srinivas, N. Ahmad, A. Surolia, *J. Biol. Chem.* **1999**, *274*, 4500 – 4503.

[65] R. Loris, P. P. G. Stas, L. Wyns, *J. Biol. Chem.* **1994**, *269*, 28722 – 28733.

[66] D. R. Bundle in *Glycosciences: Status and Perspectives* (Eds.: H.-J. Gabius, S. Gabius) Chapman & Hall, London, **1997**, pp. 311 – 331.

[67] H.-J. Gabius, R. Engelhardt, S. Rehm, F. Cramer, *J. Natl. Cancer Inst.* **1984**, *73*, 1349 – 1357.

[68] H.-J. Gabius, *Anal. Biochem.* **1990**, *189*, 91 – 94.

[69] M. Schneller, S. André, J. Cihak, H. Kaltner, H. Merkle, G. J. Rademaker, J. Haverkamp, J. Thomas-Oates, U. Lösch, H.-J. Gabius, *Cell. Immunol.* **1995**, *166*, 35 – 43.

[70] H. Kaltner, K. S. Lips, G. Reuter, S. Lippert, F. Sinowatz, H.-J. Gabius, *Histol. Histopathol.* **1997**, *12*, 945 – 960.

[71] H.-J. Gabius, B. Kohnke-Godt, M. Leichsenring, A. Bardosi, *J. Histochem. Cytochem.* **1991**, *39*, 1249 – 1256.

[72] H.-J. Gabius, B. Wosgien, M. Hendrys, A. Bardosi, *Histochemistry* **1991**, *95*, 269 – 277.

[73] S. André, C. Unverzagt, S. Kojima, X. Dong, C. Fink, K. Kayser, H.-J. Gabius, *Bioconjugate Chem.* **1997**, *8*, 845 – 855.

[74] A. T. Hagler, E. Huler, S. Lifson, *J. Am. Chem. Soc.* **1974**, *96*, 5319 – 5327.

[75] A. T. Hagler, S. Lifson, P. Dauber, *J. Am. Chem. Soc.* **1979**, *101*, 5122 – 5130.

[76] D. Mierke, H. Kessler, *Biopolymers* **1992**, *32*, 1277 – 1282.

[77] D. Mierke, H. Kessler, *Biopolymers* **1993**, *33*, 1003 – 1017.

[78] H.-C. Siebert, C.-W. von der Lieth, X. Dong, G. Reuter, R. Schauer, H.-J. Gabius, J. F. G. Vliegenthart, *Glycobiology* **1996**, *6*, 561 – 572.

[79] D. Acquotti, L. Poppe, J. Dabrowski, C.-W. von der Lieth, S. Sonnino, G. Tettamanti, *J. Am. Chem. Soc.* **1990**, *112*, 7772 – 7778.

[80] H.-C. Siebert, G. Reuter, R. Schauer, C.-W. von der Lieth, J. Dabrowski, *Biochemistry* **1992**, *31*, 6962 – 6971.

[81] L. Poppe, C.-W. von der Lieth, J. Dabrowski, *J. Am. Chem. Soc.* **1990**, *112*, 7762 – 7771.

[82] Abbreviations: 1D = one-dimensional, 2D = two-dimensional, ASF = asialofetuin, BSA = bovine serum albumin, CG = chicken galectin, CVFF = consistent-valence force field, DMSO = dimethyl sulfoxide, IgG = immunoglobulin G, Lac = lactose, MD = molecular dynamics, Mel = melibiose, MM = molecular mechanics, NOESY = nuclear Overhauser effect spectroscopy, PBS = phosphate-buffered saline, PL = poly-ʟ-lysine, RAMM = random walk molecular mechanics, ROESY = rotating-frame nuclear Overhauser enhancement spectroscopy, tr-NOE = transferred nuclear Overhauser effect, TOCSY = total coherence spectroscopy, VAA = *Viscum album* L. agglutinin (mistletoe lectin).

[83] CAT = Conformational Analysis Tool. Software details and information on further applications can be obtained from the authors.

[84] M. Frank, unpublished results.